The EMBO Journal (2005) 24, 4291–4303 | © 2005 European Molecular Biology Organization | All Rights Reserved 0261-4189/05
www.embojournal.org

THE EMBO JOURNAL

Interplay between 7SK snRNA and oppositely charged regions in HEXIM1 direct the inhibition of P-TEFb

Matjaz Barboric[1], Jiří Kohoutek[1], Jason P Price[2], Dalibor Blazek[1], David H Price[2] and B Matija Peterlin[1,*]

[1]Departments of Medicine, Microbiology, and Immunology, Rosalind Russell Medical Research Center, University of California at San Francisco, San Francisco, CA, USA and [2]Department of Biochemistry, University of Iowa, Iowa City, Iowa, USA

Transcription elongation of eukaryotic genes by RNA polymerase II depends on the positive transcription elongation factor b (P-TEFb). When sequestered into the large complex, P-TEFb kinase activity is inhibited by the coordinate actions of 7SK small nuclear RNA (7SK snRNA) and hexamethylene bisacetamide (HMBA)-induced protein 1 (HEXIM1). We found that the basic region in HEXIM1 directs its nuclear import via two monopartite and two bipartite nuclear localization sequences. Moreover, the arginine-rich motif within it is essential for its binding to 7SK snRNA, P-TEFb, and inhibition of transcription. Notably, the basic region interacts with the adjacent acidic regions in the absence of RNA. The removal of the positive or negative charges from these regions in HEXIM1 leads to its sequestration into the large complex and inhibition of transcription independently of the arginine-rich motif. Finally, the removal of the negative charges from HEXIM1 results in its subnuclear localization into nuclear speckles. We propose a model where the interplay between 7SK snRNA and oppositely charged regions in HEXIM1 direct its binding to P-TEFb and subcellular localization that culminates in the inhibition of transcription.

The EMBO Journal (2005) **24,** 4291–4303. doi:10.1038/sj.emboj.7600883; Published online 15 December 2005
Subject Categories: chromatin & transcription; RNA
Keywords: HEXIM1; nuclear speckles; P-TEFb; transcription elongation; 7SK snRNA

Introduction

The transcription of eukaryotic genes by RNA polymerase II (RNAPII) is coordinated tightly at many levels, including those of transcription elongation (Sims *et al*, 2004). Shortly after promoter clearance, the negative transcription elongation factor (N-TEF) forms a paused complex with RNAPII. The transition to robust transcription elongation depends on the positive transcription elongation factor b (P-TEFb), which is required for the expression of the human immunodeficiency virus (HIV) and most cellular protein-coding genes (Chao and Price, 2001; Barboric and Peterlin, 2005). It consists of heterodimers between a catalytic subunit, the cyclin-dependent kinase 9 (Cdk9), and one of the four C-type cyclin regulatory subunits, CycT1, CycT2a, Cyc2Tb, or CycK. When recruited to paused transcription complexes, P-TEFb phosphorylates serines at position 2 in the C-terminal domain (CTD) of the Rpb1 subunit of RNAPII and subunits of N-TEF, resulting in the efficient elongation and cotranscriptional processing of nascent pre-mRNA molecules.

Besides the active, heterodimeric form, P-TEFb exists in a larger, catalytically inactive complex in cells in which the 7SK small nuclear RNA (7SK snRNA) was found initially (Nguyen *et al*, 2001; Yang *et al*, 2001). In addition to P-TEFb and 7SK snRNA, this large complex contains the hexamethylene bisacetamide (HMBA)-induced protein 1 (HEXIM1) (Michels *et al*, 2003; Yik *et al*, 2003) that has been identified previously as a protein whose expression is induced by HMBA in vascular smooth muscle cells (Kusuhara *et al*, 1999). Growing body of evidence suggests that the coordinated actions of 7SK snRNA and HEXIM1 result in the inhibition of P-TEFb (Yik *et al*, 2003; Michels *et al*, 2004). In a proposed model, 7SK snRNA binds the basic region in HEXIM1 (BR), which is the prerequisite for the interaction between the C-terminus of HEXIM1 and CycT1, culminating in the inactivation of P-TEFb (Michels *et al*, 2004; Li *et al*, 2005; Schulte *et al*, 2005). Notably, another HEXIM1-related protein, HEXIM2, binds and inhibits P-TEFb in the presence of 7SK snRNA (Byers *et al*, 2005; Yik *et al*, 2005). Moreover, the assembly of the large complex is facilitated due to the homo- and hetero-oligomerization of HEXIM1 and HEXIM2 (Dulac *et al*, 2005; Li *et al*, 2005; Yik *et al*, 2005). Finally, the ratio between active and inactive P-TEFb complexes controls cell growth. For example, several growth signals release P-TEFb from the inactive complex in cardiac hypertrophy in mice, a disease characterized by the enlargement of cardiac myocytes due to a global increase in mRNA and protein contents (Sano *et al*, 2002).

In addition to binding 7SK snRNA, the BR is required for the nuclear import of HEXIM1 (Ouchida *et al*, 2003). In principle, nucleocytoplasmic transport occurs through the nuclear pore complexes (NPCs) and is carried out by karyopherins, which include importins and exportins (Weis, 2003). Most karyopherins bind the topogenic sequences for protein transport directly. For example, importin β translocates the HIV-1 regulatory proteins Tat and Rev by binding their arginine-rich nuclear localization sequences (NLSs) directly (Truant and Cullen, 1999). In contrast, importin β can also bind the classical, lysine-rich, NLS-containing cargos via an adaptor protein, importin α. This latter mechanism constitutes the classical nuclear import pathway, in which importin α binds the NLS and importin β docks the ternary complex at

*Corresponding author. Box 0703, 3rd and Parnassus Aves, San Francisco, CA 94143-0703, USA. Tel.: +1 415 502 1902; Fax: +1 415 502 1901; E-mail: matija@itsa.ucsf.edu

Received: 21 February 2005; accepted: 2 November 2005; published online: 15 December 2005

the NPC. Classical NLSs are typified by either a single basic cluster (monopartite NLS) or two interdependent basic clusters separated by 10–12 amino-acid linker region (bipartite NLS). The proposed consensus sequences for monopartite NLS comprises KKxK, whereas the consensus sequence for the bipartite NLS is $KRx_{10\text{-}12}KRxK$, in which the shorter basic cluster precedes the longer one (Weis, 2003).

At present, little is known about the detailed mechanisms that govern the nuclear import of HEXIM1. Moreover, the requirement for 7SK snRNA in turning HEXIM1 into a P-TEFb inhibitor is understood poorly. In this study, we present a comprehensive analysis of the central region in HEXIM1 that consists of oppositely charged BR and adjacent acidic region (AR). Based on our findings, we propose a scenario in which the interplay between 7SK snRNA and the oppositely charged regions dictate nuclear localization of HEXIM1 and binding to P-TEFb, leading to its inactivation and thus inhibition of transcription elongation.

Results

BR in HEXIM1 contains multiple predicted NLSs

Primary structure analysis of HEXIM1 showed that 14% of the protein consists of basic and 21% of acidic residues. In total, 54% of the former and 63% of the latter are clustered in several regions with high probability of low structural complexity, among which one is especially rich in basic and another in acidic residues, thus constituting BR and AR, respectively (Figure 1A). We first focused on the BR in HEXIM1 from positions 150 to 177, which includes BR1 and BR2, and determined that it is conserved among HEXIM proteins from different species (Figure 1B). Of note, the BR2 from positions 175 to 177 in HEXIM1 is conserved in the mouse ortholog but absent in other HEXIM proteins. Next, we analyzed the BR in detail and identified nearly perfect consensus sequences for two monopartite and two bipartite NLSs (Figure 1C).

Two monopartite and two bipartite NLSs in the BR of HEXIM1 direct its nuclear import

To understand the nuclear import of HEXIM1, we disrupted the predicted NLSs by constructing a series of FLAG epitope-tagged HEXIM1 (f.Hex1) proteins, in which the selected basic clusters (B1–6) were replaced with alanines individually or in combination (Figure 1D), and determined their subcellular localizations by using indirect immunofluorescence visualized by confocal microscopy in transiently transfected HeLa cells (Figure 2). In agreement with a previous report (Ouchida *et al*, 2003), we observed a nuclear localization for f.Hex1, which was converted into a cytoplasmic one upon the deletion of the BR (f.Hex1ΔBR; Figure 2A, compare images 2 and 3). Critically, only when we disrupted all four selected basic clusters at the same time (f.Hex1mB1256) did we observe a cytoplasmic localization, similar to the localization of the mutant f.Hex1ΔBR protein (Figure 2A, compare image 4 with images 2 and 3). Thus, four distinct NLSs in HEXIM1 direct its nuclear import.

To decode monopartite and bipartite NLSs, we next examined subcellular localizations of mutant f.Hex1 proteins with individual, double, or triple disruptions of the basic clusters. All of these proteins were nuclear (Figure 2A, images 5–7 and data not presented), except for the mutant f.Hex1mB256 protein, whose nuclear localization was reduced modestly (Figure 2A, image 8). Thus, the mutant f.Hex1mB156 and f.Hex1mB126 proteins still contain functional first and second predicted monopartite NLSs, respectively, whereas in the mutant f.Hex1mB256 protein, the first predicted monopartite

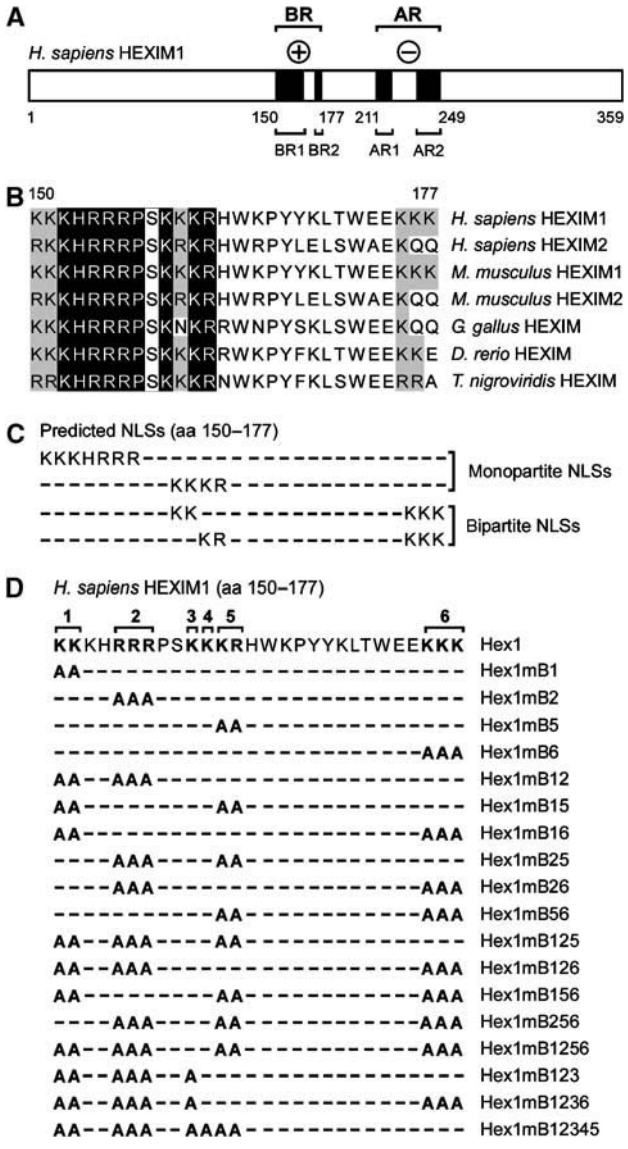

Figure 1 BR in HEXIM1 contains multiple predicted NLSs. (**A**) HEXIM1 protein is presented as a white rectangle. Black boxes represent two basic (BR; BR1 and BR2) and two acidic (AR; AR1 and AR2) regions and the encircled signs above them represent the charge of these regions. The sequence numberings correspond to the N-terminus, the boundaries of the BRs and ARs, and the C-terminus, respectively. (**B**) Alignment of the BRs of human, mouse, chicken, zebrafish, and fish HEXIM1 and HEXIM2 proteins. Reverse type indicates basic amino-acid identity whereas shaded boxes indicate basic amino-acid similarity. (**C**) Predicted monopartite and bipartite NLSs within the BR in HEXIM1 is presented. (**D**) HEXIM1 proteins used in the first part of the study. Hex1 represents the primary amino-acid sequence of the BR in HEXIM1, which was a subject to site-directed mutagenesis. Numbers above this sequence indicate a disruption of the corresponding basic cluster. The names of wild-type and mutant Hex1 proteins are presented on the right-hand side of the panel. A capital letter B symbolizes basic cluster, whereas small letter m symbolizes the replacement of corresponding basic clusters with alanines.

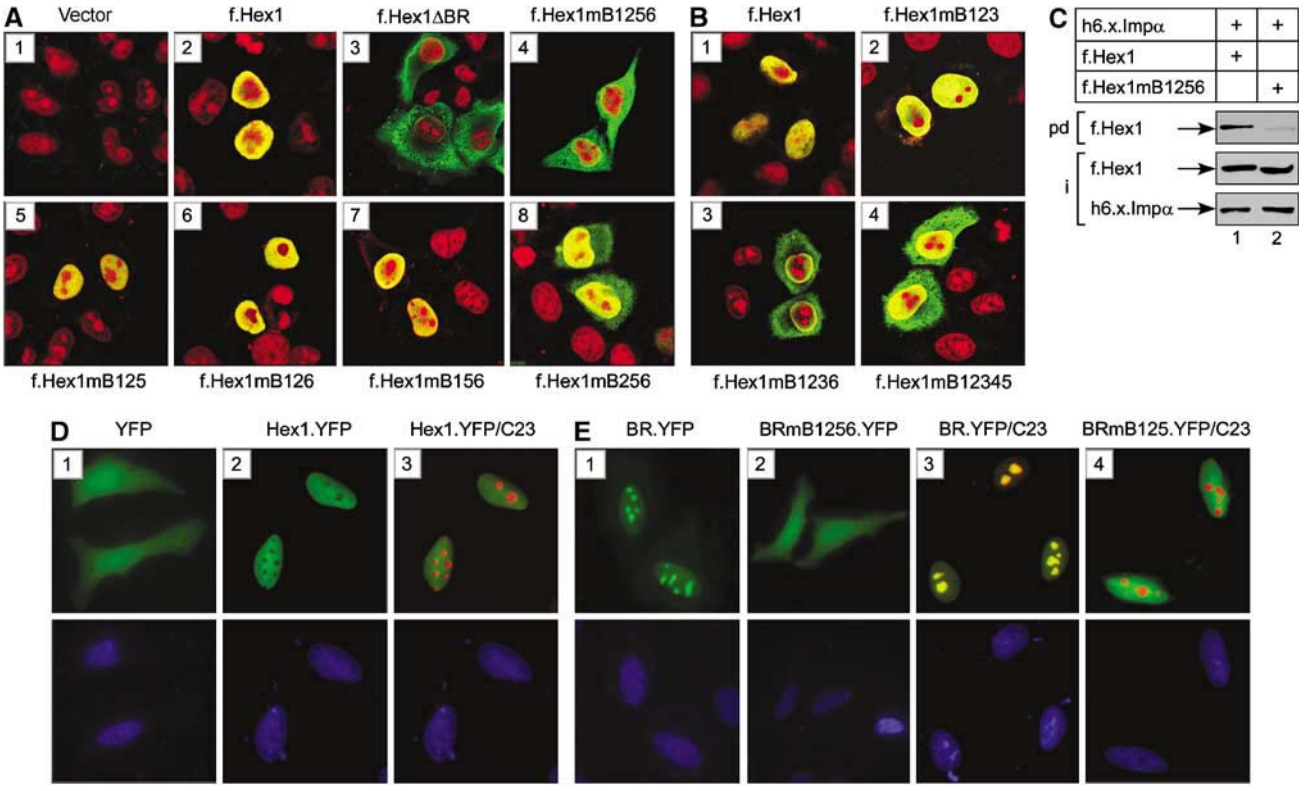

Figure 2 Four distinct NLSs direct nuclear import of HEXIM1. (**A, B**) f.Hex1 proteins (green) that were expressed in HeLa cells are indicated above and below the microscopic images. Cell nuclei were visualized by propodium iodide (PI; red). The images depict the merge of the f.Hex1 and PI images. (**C**) HeLa cell lysates, which expressed f.Hex1 or f.Hex1mB1256 from corresponding plasmid effectors (10 μg), were incubated with h6.x.Impα as indicated. Arrows to the left indicate bound f.Hex1 proteins (pd) and 10% inputs (i) of the proteins used in the assay, respectively. (**D**) YFP (image 1) and Hex1.YFP (images 2 and 3) proteins (green) were expressed in HeLa cells. The panel marked Hex1.YFP/C23 depict the merge of the Hex1.YFP (green) and C23 (red) images. (**E**) BR.YFP proteins (green) that were expressed in HeLa cells are indicated above the microscopic images. Where indicated, the images depict the merge of the respective BR.YFP (green) and C23 (red) images. Lower parts of the panels D and E indicate the cell nuclei of which the DNA was counterstained by DAPI (blue).

NLS was disrupted partially. Similarly, when contrasted to the nuclear localization of the mutant f.Hex1mB126 protein, the partially cytoplasmic localization of the mutant f.Hex1mB1236 protein (Figure 2A and B, compare images 6 and 3, respectively) confirms the presence of the second predicted monopartite NLS. Next, the nuclear localizations of the mutant f.Hex1mB125 protein and the cytoplasmic localization of the mutant f.Hex1mB1256 protein indicate the activity of the first predicted bipartite NLS, which comprises the basic clusters B34 and B6, separated by a spacer of 14 residues. To address further the importance of the basic cluster B6 and thus the existence of the second predicted bipartite NLS, we constructed another series of mutant f.Hex1 proteins and determined their subcellular localizations (Figure 2B). Indeed, the nuclear localization of the mutant f.Hex1mB123 protein was affected greatly by the disruption of the basic cluster B6 (Figure 2B, compare images 2 and 3), suggesting the activity of the second predicted bipartite NLS. Finally, we observed a partial cytoplasmic localization of the mutant f.Hex1mB12345 protein (Figure 2B, image 4), demonstrating that the basic cluster B6 is not a monopartite NLS. We conclude that two monopartite and two bipartite NLSs in HEXIM1 direct its nuclear import. Moreover, the basic clusters B1, B45, and B6 do not constitute fully functional monopartite NLSs. Rather, the former two are part of both monopartite NLSs whereas the latter form the second basic cluster of the two bipartite NLSs.

The first step in the classical nuclear import pathway is the interaction between importin α and the classical monopartite or bipartite NLSs (Weis, 2003). To examine if HEXIM1 binds importin α *in vitro* and whether this binding depends on its NLSs, we purified bacterially expressed importin α as a His_6-Xpress epitope-tagged protein (h6.x.Impα) and incubated it with HeLa cell lysates, which contained the f.Hex1 or mutant f.Hex1mB1256 proteins. The wild-type f.Hex1 protein bound h6.x.Impα efficiently whereas the mutant f.Hex1mB1256 protein did not (Figure 2C, compare lanes 1 and 2). Also, the inputs of f.Hex1 proteins and h6.x.Impα were comparable in the binding reactions (Figure 2C, lower panel). Thus, HEXIM1 binds importin α via its NLSs *in vitro*.

Two monopartite and two bipartite NLSs of HEXIM1 direct the nuclear import of the enhanced yellow fluorescent protein

To confirm the identification of the four distinct NLSs in HEXIM1, we used a heterologous system, in which we fused the cDNAs of HEXIM1 and a plethora of the wild-type or the mutated BRs described above to the N-terminus of the enhanced yellow fluorescent protein (YFP). Subcellular localizations of these chimeras were determined by using immunofluorescence microscopy of transiently transfected HeLa cells (Figure 2D and E). In these experiments, DAPI staining of the DNA was employed throughout to visualize the nuclei of the cells. As expected, the fusion between the

HEXIM1 and YFP proteins (Hex1.YFP) resulted in the nuclear localization of the Hex1.YFP chimera, whereas the YFP protein itself displayed a nuclear and cytoplasmic localization (Figure 2D, compare images 1 and 2). Notably, since it failed to colocalize with the nucleolar marker C23, the Hex1.YFP protein was excluded from nucleoli and was present exclusively in the nucleoplasm (Figure 2D, image 3).

Finally, we examined the subcellular localizations of the BR.YFP fusion proteins. Localizations of these chimeras correlated entirely with the ones in which the BR was part of the f.Hex1 proteins (Figure 2D and E and Supplementary Figure 1). As expected, only the wild-type BR.YFP but not the mutant BRmB1256.YFP chimera was imported into the nucleus efficiently (Figure 2E, images 1 and 2). Interestingly, the presence of the evolutionary conserved arginine-rich motif (ARM) (position 154–156 in HEXIM1; basic cluster B2) within the BR.YFP protein caused a predominantly nucleolar localization whereas its disruption led to a nucleoplasmic localization (Figure 2E, images 3 and 4 and Supplementary Figure 1). Thus, the four distinct NLSs function fully when fused to the heterologous protein. Taken together, we conclude that two monopartite and two bipartite NLSs within the evolutionary conserved BR direct the nuclear import of HEXIM. Moreover, when present in the BR.YFP chimera, an intact ARM constitutes a nucleolar localization sequence (NoLS) that was not observed functional within the Hex1.YFP chimeric protein, which was localized in the nucleoplasm.

ARM in the BR1 is essential for the binding of HEXIM1 to 7SK snRNA

The binding between 7SK snRNA and the BR in HEXIM1 is a prerequisite for its ability to inhibit P-TEFb (Michels *et al*, 2004; Yik *et al*, 2004). To map the surfaces on HEXIM1 critical for binding 7SK snRNA, we took advantage of the mutant HEXIM1 proteins with disrupted basic clusters (B1, 2, 5, 6; see Figure 1D) and performed electrophoretic mobility shift assays (EMSAs; Figure 3A). For these experiments, we pur-

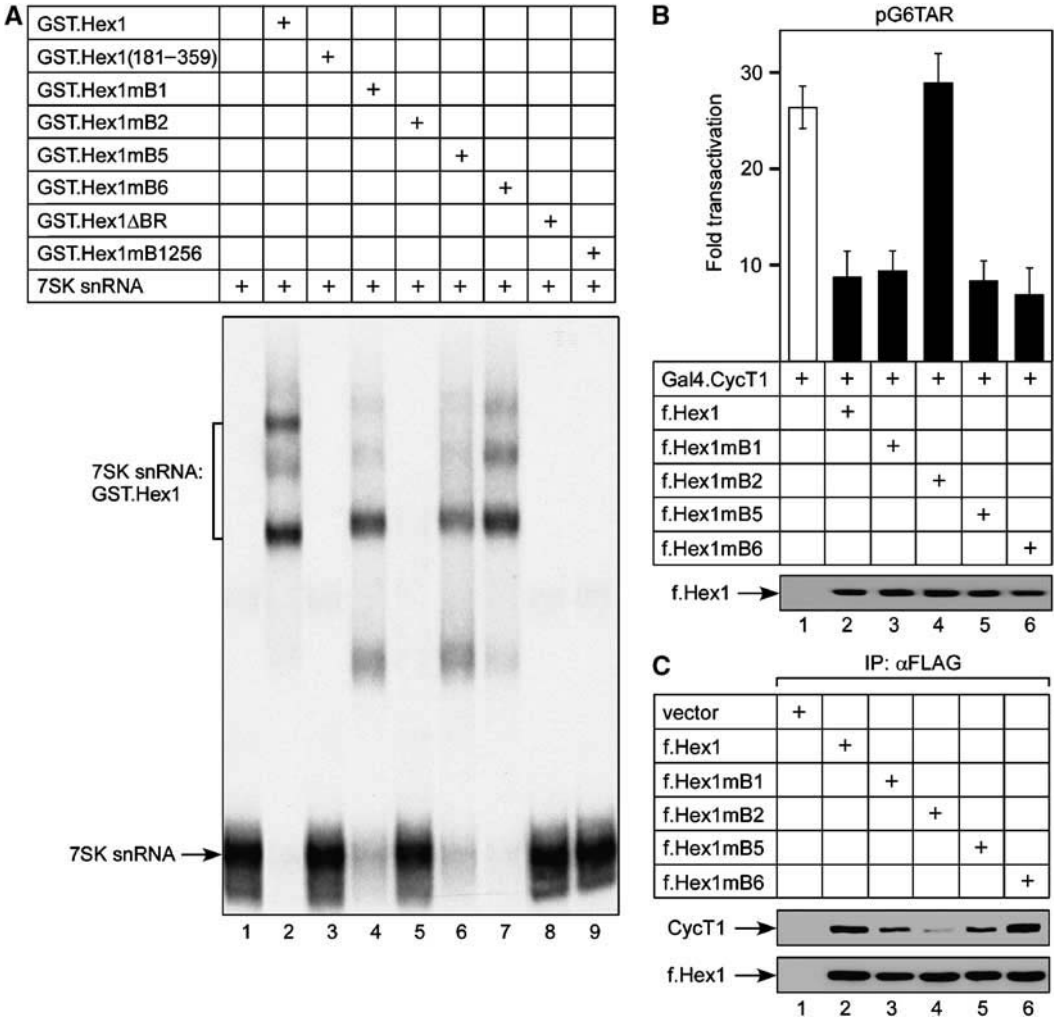

Figure 3 The disruption of the ARM in HEXIM1 disables its binding to 7SK snRNA *in vitro* and inhibition of transcription and binding to P-TEFb *in vivo*. (**A**) Chimeric GST.Hex1 proteins are indicated above the autoradiograph. α-^{32}P-labeled 7SK snRNA was present in all reactions. Arrow to the left indicates the free 7SK snRNA probe and the presence of 7SK snRNA:GST.Hex1 RNA–protein complexes is bracketed. (**B**) HeLa cells expressed plasmid reporter pG6TAR (0.4 μg; bars 1–6). Proteins that were coexpressed from corresponding plasmid effectors (Gal4.CycT1, 0.6 μg; f.Hex1, 0.8 μg) with the plasmid reporter are presented below CAT data. The lower panels present the expression of f.Hex1 proteins as indicated by the arrow. (**C**) f.Hex1 proteins that were expressed in HeLa cells from corresponding plasmid effectors (10 μg; lanes 2–6) and immunoprecipitated by anti-FLAG M2 beads are indicated above the Western blots. Arrows to the left indicate the bound P-TEFb and the amounts of immunoprecipitated f.Hex1 proteins, respectively.

ified bacterially expressed chimeric GST.HEXIM1 (GST.Hex1) proteins and incubated them with the *in vitro* transcribed and α-^{32}P-labeled 7SK snRNA. As expected, the wild-type GST.Hex1 chimera bound 7SK snRNA efficiently and the N-terminal deletion mutant of GST.Hex1 (GST.Hex1 (181–359)) or the GST.Hex1ΔBR fusion proteins did not, confirming the requirement of the BR for this binding (Figure 3A, compare lane 2 with lanes 3 and 8). Importantly, the mutant GST.Hex1mB2 chimera, where the ARM was disrupted, failed to bind 7SK snRNA (Figure 3A, lane 5). In contrast, the bindings between 7SK snRNA and the mutant GST.Hex1mB1 and GST.Hex1mB5 chimeras, respectively, decreased slightly when compared to the wild-type GST.Hex1 fusion protein, whereas the mutant GST.Hex1mB6 chimera retained the ability to bind 7SK snRNA fully (Figure 3A, lanes 4, 6, and 7). Predictably, when all four basic clusters were disrupted, the mutant GST.Hex1mB1256 chimera did not bind 7SK snRNA (Figure 3A, lane 9). We conclude that the ARM in the BR1 is essential for its binding to 7SK snRNA and that the basic clusters B1 and B5 contribute to these protein–RNA interactions whereas the basic cluster B6 does not.

ARM in the BR1 is essential for HEXIM1 to inhibit transcription and bind to P-TEFb

To extend our *in vitro* binding studies presented in Figure 3A, we addressed the importance of the ARM for the ability of HEXIM1 to bind and inhibit P-TEFb in cells. We performed transcriptional assays followed by binding studies using transiently transfected HeLa cells (Figure 3B and C). To monitor the transcriptional activation by P-TEFb and the inhibitory effects of HEXIM1 proteins on this activation, we used the system, consisting of a plasmid reporter pG6TAR, which contains six Gal4 DNA-binding sites positioned upstream of the HIV-1 long terminal repeat (HIV LTR), followed by the CAT reporter gene, and the chimeric Gal4.CycT1 protein. Its recruitment to the pG6TAR promoter activates transcription that depends on the kinase activity of P-TEFb (Taube *et al*, 2002).

When we expressed Gal4.CycT1 chimera together with pG6TAR in HeLa cells, the levels of CAT activity increased 28-fold over the basal levels, whereas the coexpression of the wild-type f.Hex1 protein decreased this activity to nine-fold (Figure 3B, compare bars 1 and 2). Critically, the disruption of the ARM rendered the mutant f.Hex1mB2 protein largely inactive (Figure 3B, bar 3). Moreover, the disruptions of the basic clusters B1, B5, and B6 had no effect, since the corresponding mutant f.Hex1 proteins inhibited the activation of transcription by the Gal4.CycT1 chimera similarly to the wild-type f.Hex1 protein (Figure 3B, bars 3, 5, and 6). We observed the same results when we monitored effects of these mutant f.Hex1 proteins on Tat transactivation of the HIV LTR (data not presented). Also, levels of the f.Hex1 proteins were comparable (Figure 3B, lower panel). Thus, the ARM in the BR1 of HEXIM1 is critical for its inhibition of transcription in cells.

To address the requirements of the basic clusters for its binding to P-TEFb, we performed immunoprecipitation assays (Figures 3C). We again employed the wild-type or mutant f.Hex1 proteins tested in Figure 3B and found predictably that the wild-type f.Hex1 protein bound P-TEFb in cells (Figure 3C, lane 2). In contrast, the mutant f.Hex1mB2 protein bound P-TEFb poorly, whereas the disruptions of basic clusters B1, B5, and B6 had only modest to no effects on the binding (Figure 3C, lanes 3–6). Also, levels of the f.Hex1 proteins in the immunoprecipitations were comparable (Figure 3C, lower panel). Overall, we conclude that the ability of HEXIM1 to inhibit transcription and bind P-TEFb depends on its ARM.

BR and AR mediate the interaction between the N- and C-terminal regions of HEXIM1 in the absence of RNA

Thus far, our findings suggested that the BR performs two functions, nuclear import and 7SK snRNA binding, which results in P-TEFb binding and inhibition of transcription. However, as presented in Figure 1A, the BR is followed by AR, consisting of AR1 and AR2. Owing to the close proximity of BR and AR, their high likelihood of low structural complexity and opposite charge, we hypothesized that they might interact with one another and thus lead to an autoinhibitory conformation of HEXIM1 that would be refractory to P-TEFb binding. Moreover, we postulated that this conformation could be changed by the interaction between the BR and 7SK snRNA, resulting in a conformation of HEXIM1 that would allow the binding and inhibition of P-TEFb.

To address this hypothesis, we examined if the N- and C-terminal regions of HEXIM1 interact *in vitro* and whether this interaction is mediated by the BR, AR, and the presence of RNA (Figure 4). For these binding experiments, we used the mutant HEXIM1 proteins that either contain or lack the BR and AR, respectively (Figure 4A). The two bacterially expressed C-terminal deletion mutant HEXIM1 proteins were purified as GST chimeras and the three N-terminal deletion mutant HEXIM1 proteins were expressed as His_6-Xpress epitope-tagged (h6.x.Hex1) chimeras *in vitro* using the rabbit reticulocyte lysate.

First, we asked whether the N- and C-terminal regions of HEXIM1 interact (Figure 4B). Indeed, the mutant GST.Hex1(1–180) and h6.x.Hex1(181–359) proteins bound each other in the presence of RNase A (Figure 4B, lanes 3 and 4). In contrast, the mutant GST.Hex1(1–150) chimera, which lacked the BR, failed to bind the mutant h6.x.Hex1(181–359) protein in the presence of RNase A (Figure 4B, lanes 1 and 2). Also, the inputs of the mutant h6.x.Hex1(181–359) protein were comparable in the binding reactions (data not presented). Thus, the interaction between the N- and C-terminal regions of HEXIM1 *in vitro* is mediated by the BR and occurs in the absence of RNA.

Moreover, we addressed the importance of the adjacent AR for the binding between the N- and C-terminal regions of HEXIM1 (Figure 4C). We performed the binding between the mutant GST.Hex1(1–180) chimera with the intact BR and the series of the N-terminal deletion mutant h6.x.Hex1 proteins as described above. Predictably, the mutant GST.Hex1(1–180) chimera bound the mutant h6.x.Hex1(181–359) protein in the presence of RNase A (Figure 4C, lanes 1 and 2). Critically, the mutant GST.Hex1(1–180) chimera failed to bind the mutant h6.x.Hex1(255–359) protein, which lacked the AR (Figure 4C, lanes 5 and 6). In contrast, the binding was not affected with the mutant h6.x.Hex1(206–359) protein, which still retained the AR (Figure 4C, lanes 3 and 4). Also, the inputs of the mutant h6.x.Hex1 proteins were comparable in the binding reactions (Figure 4C, lanes 7–9). Overall, we conclude that

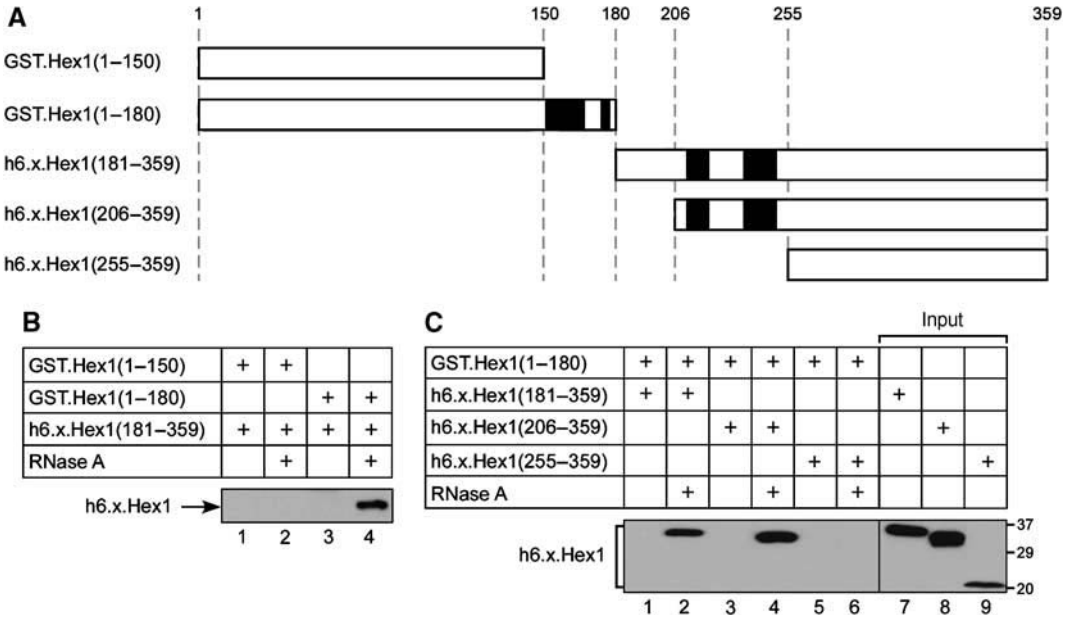

Figure 4 The interaction between the BR and AR within HEXIM1 *in vitro* is abolished in the presence of RNA. (**A**) The mutant GST.Hex1 and h6.x.Hex1 proteins are presented as white rectangles. Black boxes depict BR and AR as in Figure 1A. The numberings above the schematic correspond to the N- and/or C-terminal boundaries of the proteins. The names of the proteins are presented on the left-hand side of the panel. (**B, C**) Chimeric GST.Hex1 proteins were incubated with the mutant h6.x.Hex1 protein in the presence or absence of RNase A as indicated above the Western blot. Arrow to the left in panel B indicates the bound h6.x.Hex1 protein. In the panel C, the h6.x.Hex1 proteins are bracketed. Left part of the panel (lanes 1–6) represents the bound h6.x.Hex1 proteins, whereas the right part of the panel (lanes 7–9) represents the 20% inputs of the proteins used in the assay. Numbers to the right indicate relative molecular mass markers (in kDa).

the interaction between the N- and C-terminal regions of HEXIM1 *in vitro* depends on the BR and AR and that the presence of RNA prevents this binding.

Disruption of the BR in HEXIM1 renders the ARM dispensable for inhibition of transcription

To this end, we established that the BR and AR bind each other in the absence of RNA. These observations support our hypothetical model, where 7SK snRNA binds the ARM within the BR to alter a conformation of HEXIM1 that would lead to the binding and inhibition of P-TEFb. Thus, one could predict that the removal of either a positive charge from the BR or the negative charge from the AR would result in this changed conformation, thus mimicking artificially the requirement for 7SK snRNA for the inhibition of P-TEFb.

To test this prediction, we first took advantage of the mutant Hex1mB1256 protein, in which the majority of the positive charge within the BR was removed (Figure 1C) and asked whether it could bind and inhibit P-TEFb in cells (Figure 5). To do so, we used the same strategy as employed in Figure 4B. Since the mutant f.Hex1mB1256 protein localizes in the cytoplasm (Figure 2A, image 4), we fused the NLS of the SV-40 large T antigen to its N-terminus to create the mutant f.NLS.Hex1mB1256 chimera, which resulted in its nuclear localization (Figure 5B, compare images 1 and 2). Strikingly, the mutant f.NLS.Hex1mB1256 chimera inhibited the activation of transcription by the Gal4.CycT1 chimera equivalently to the wild-type f.Hex1 protein, whereas the mutant f.Hex1mB1256 protein had no effect, most likely due to its cytoplasmic localization (Figure 5A, compare bar 4 with bars 1–3). Levels of the mutant f.Hex1 proteins were comparable (Figure 5A, lower panel). Next, we performed immunoprecipitation assays as described in Figure 3C and found that the mutant f.NLS.Hex1mB1256 chimera bound P-TEFb in cells (Figure 5C, lane 3). Notably, the mutant GST.Hex1mB1256 chimera did not bind 7SK snRNA *in vitro* (Figure 3A, lane 9).

Collectively, these results suggested that the mutant f.NLS.Hex1mB1256 chimera gets sequestered into the large complex independently of ARM and that the 7SK snRNA is not required for this event in cells. To test these notions, we performed a glycerol gradient sedimentation analysis to observe the small and large P-TEFb complexes in cells (Figure 5D). Indeed, we observed two distinct pools of endogenous P-TEFb and HEXIM1 complexes in HeLa cells (Figure 5D, panels a and b). As expected, the wild-type f.Hex1 protein was sequestered into the large complex efficiently whereas the mutant f.Hex1mB2 with a disrupted ARM was not (Figure 5D, panels c and d). Importantly, the additional removal of positive charge from the BR of the mutant f.Hex1mB2 rescued the sequestration into the large complex, since we detected the mutant f.NLS.Hex1mB1256 chimera in it (Figure 5D, panel e). Critically, the destruction of 7SK snRNA by RNase A did not result in a disappearance of the mutant f.NLS.Hex1mB1256 chimera from the large complex, which occurred in the case of the wild-type f.Hex1 protein (Figure 5D, panels f and g). Thus, the removal of positive charge from the BR in HEXIM1 alleviates the requirement for the ARM to bind and inhibit P-TEFb. The fact that the sequestration of the mutant f.NLS.Hex1mB1256 protein was insensitive to RNase A treatment suggests that this mutant HEXIM1 protein inhibits P-TEFb independently of 7SK snRNA. Overall, we conclude that the interaction between the 7SK snRNA and the BR in HEXIM1 via the ARM is critical for the HEXIM1 inhibitory function.

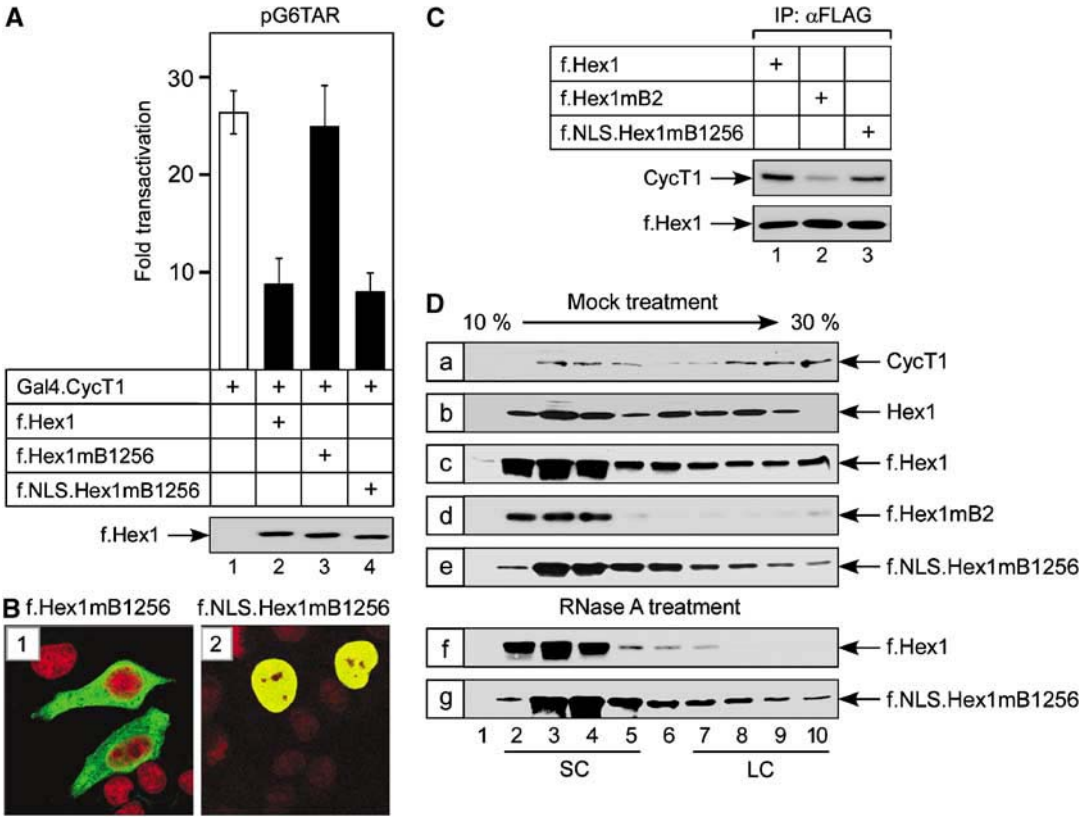

Figure 5 The disruption of the BR in HEXIM1 enables the ARM-independent inhibition of transcription and binding to P-TEFb *in vivo*. (**A**) HeLa cells expressed plasmid reporter pG6TAR (0.4 μg; bars 1–6). Proteins that were coexpressed from corresponding plasmid effectors (Gal4.CycT1, 0.6 μg; f.Hex1, 0.8 μg) with the plasmid reporter are presented below CAT data. The lower panel presents the expression of f.Hex1 proteins as indicated by the arrow. (**B**) f.Hex1 proteins that were expressed in HeLa cells from corresponding plasmid effectors (1 μg) are indicated above and below the microscopic images. f.Hex1 proteins (green) and nuclei (red) were visualized by laser confocal microscopy. (**C**) f.Hex1 proteins that were expressed in HeLa cells from corresponding plasmid effectors (10 μg; lanes 1–3) and immunoprecipitated by anti-FLAG M2 beads are indicated above the Western blots. Arrows to the left indicate bound P-TEFb and the amounts of immunoprecipitated f.Hex1 proteins, respectively. (**D**) Total cell lysates of untransfected HeLa cells and those that expressed the indicated f.Hex1 proteins were subjected to glycerol gradient (10–30%) sedimentation analysis. The lysates were mock or RNase A treated as indicated above the Western blots. Arrows to the right indicate the presence of endogenous CycT1 and HEXIM1 (Hex1) proteins, and f.Hex1 proteins that were expressed from corresponding plasmid effectors (6 μg). Numberings below the Western blots correspond to particular fractions obtained from the sedimentation analysis. SC and LC indicate fractions containing the small and large complexes, respectively.

Moreover, this dependency on the 7SK snRNA could be overcome by disrupting the BR, suggesting that the postulated autoinhibitory conformation of HEXIM1 is changed into the one that could bind and inhibit P-TEFb.

Disruption of the AR1 in HEXIM1 renders the ARM dispensable for inhibition of transcription

To substantiate this model further, we addressed the significance of the AR for the inhibition of P-TEFb in cells (Figure 6). We analyzed the AR in detail and determined that the AR1 from positions 211 to 219 is conserved among HEXIM1 and HEXIM2 proteins from different species, whereas the AR2 from positions 234 to 249 is absent from human and mouse HEXIM2 proteins (Figure 6A). Next, we designed a reciprocal experiment to the one presented in Figure 5 by constructing a series of mutant f.Hex1 proteins, in which the selected acidic clusters (A1–3) were disrupted by alanines individually or in combination (Figure 6A, lower panel) in the context of the wild-type f.Hex1 and the mutant f.Hex1mB2 proteins. We argued that the removal of the negative charge from the AR could alleviate the requirement for the ARM and thus 7SK snRNA binding, turning the inactive mutant f.Hex1mB2 protein into a P-TEFb inhibitor. First, we tested the ability of these mutant f.Hex1 proteins to inhibit transcriptional activation by P-TEFb in cells using the same strategy as presented in Figures 3 and 5. Indeed, when we removed the negative charge from the AR1, the inhibitory activity of the mutant f.Hex1mB2 protein was restored (Figure 6B, bars 1–3). However, the individual disruptions of the acidic clusters A1 and A2 within the AR1 or the disruption of the entire AR2 had no effect (Figure 6B, bars 4–6). Importantly, the alanine mutagenesis of the AR1 and AR2 in the context of the wild-type f.Hex1 protein had no effect since both mutant proteins inhibited transcriptional activation by the Gal4.CycT1 chimera (Figure 6B, bars 7–9). Also, the levels of the f.Hex1 proteins were comparable (Figure 6B, lower panel). Thus, similar to the removal of positive charge, the absence of the negative charge in the evolutionary conserved AR1 alleviates the need for the ARM and turns the mutant f.Hex1mB2 protein into a transcriptional inhibitor.

To explore further the mechanism by which the mutant f.Hex1mB2A12 protein with a disrupted AR1 inhibited transcription, we tested whether the disruption of ARs would

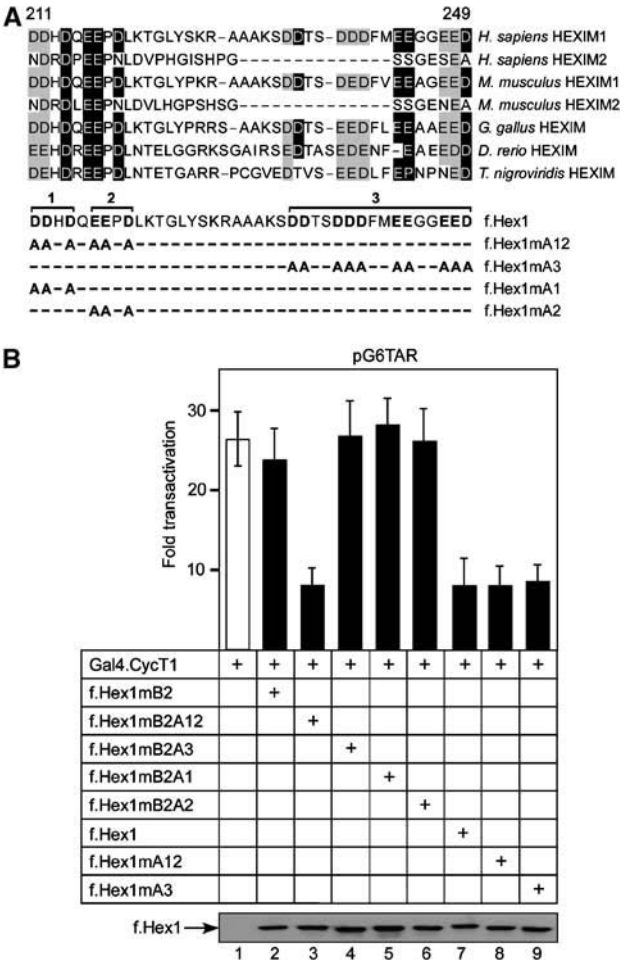

Figure 6 The disruption of the AR1 in HEXIM1 enables the ARM-independent inhibition of transcription. (**A**) Alignment of human, mouse, chicken, zebrafish, and fish HEXIM1 and HEXIM2 proteins and f.Hex1 proteins used in the study. The sequence numberings correspond to the boundaries of the ARs in HEXIM1. Reverse type indicates acidic amino-acid identity, whereas shaded boxes indicate acidic amino-acid similarity. The lower panel represents the primary amino-acid sequence of the AR in HEXIM1, which was a subject to site-directed mutagenesis. Numbers above this sequence indicate a disruption of the corresponding acidic cluster. The names of Hex1 proteins are presented on the right-hand side of the panel. A capital letter A symbolizes acidic cluster, whereas a small letter m symbolizes the replacement of corresponding acidic clusters with alanines. (**B**) HeLa cells expressed plasmid reporter pG6TAR (0.4 μg; bars 1–9). Proteins that were coexpressed from corresponding plasmid effectors (Gal4.CycT1, 0.6 μg; f.Hex1, 0.8 μg) with the plasmid reporter are presented below CAT data. The lower panel presents the expression of f.Hex1 proteins as indicated by the arrow.

affect 7SK snRNA binding (Figure 7A). We expressed and purified the wild-type and the mutant GST.Hex1 proteins from *Escherichia coli* and performed EMSAs as described in Figure 3A. Predictably, whereas all the mutant GST.Hex1 chimeras with intact ARM in HEXIM1 bound 7SK snRNA, those with the disrupted ARM failed to bind 7SK snRNA similarly (Figure 7A, lanes 1–7). Next, we asked whether the disrupted acidic clusters alleviate the requirement for the ARM in HEXIM1 to bind P-TEFb (Figure 7B). We performed a GST pull-down assay in which we took advantage of the GST.Hex1 chimeras and used them to pull down P-TEFb from a total cell lysate of HeLa cells that were treated with actinomycin D to release P-TEFb from the 7SK snRNA-bound HEXIM1. Whereas the mutant GST.Hex1mB2 failed to bind P-TEFb efficiently, the mutant GST.Hex1 proteins with the disrupted AR1 and AR2 bound P-TEFb similarly to the wild-type GST.Hex1 chimera (Figure 7B, lanes 1–4). Also, the input levels of the GST.Hex1 and P-TEFb proteins in the binding reactions were comparable (Figure 7B, lower panel). Since the mutant f.Hex1mB2A12 protein bound P-TEFb and inhibited transcription in cells without the ability to bind 7SK snRNA *in vitro*, we asked whether it gets sequestered into the large complex in cells in the ARM- and 7SK snRNA-independent manner. We again employed the glycerol gradient sedimentation analysis (Figure 7C). Indeed, we found that the disruptions of both AR1 and AR2 restored the ability of the mutant f.Hex1mB2 protein to be sequestered into the large complex (Figure 7C, panels a and b). Importantly, this sequestration was not affected by the destruction of 7SK snRNA by RNase A (Figure 7C, panels c and d). Finally, we found that the disruptions of ARs within the mutant f.Hex1 and f.Hex1mB2 proteins did not affect their oligomerization properties (Supplementary Figure 2 and data not presented). Overall, we conclude that the removal of negative charges from the ARs renders the ARM in HEXIM1 dispensable for its incorporation into the large complex and the binding to P-TEFb. However, only the disruption of the AR1 leads to the inhibitory function of f.Hex1mB2.

Disruption of the AR1 in HEXIM1 leads to its localization into nuclear speckles

To address the latter phenomenon, we lastly turned our attention to subcellular localizations of the HEXIM1 proteins with the disrupted ARs (Figure 8). We fused the corresponding cDNAs to the N-terminus of the YFP protein and performed a subcellular localization analysis of these chimeric proteins as described in Figure 2. As expected, the localization of the mutant Hex1mB2.YFP chimeric protein that has the disrupted ARM was nucleoplasmic (Figure 8A, image 1). Surprisingly, the disruption of the AR1 led to the speckled nuclear localization of the mutant Hex1mB2A12.YFP protein, whereas the disruption of the AR2 had no effect (Figure 8A, images 2 and 3). In addition, the same phenotype was observed when we disrupted the ARs in the context of the wild-type Hex1.YFP chimeras (data not presented). Thus, these findings correlate nicely with the inhibitory properties of the mutant f.Hex1mB2 proteins that have disrupted AR1 and AR2 and suggest that subnuclear localization influences their function.

To disclose the identity of the Hex1mB2A12.YFP speckled localization, we next attempted to colocalize it with several markers of distinct subnuclear structures (Figure 8B). Speckled localization was highly reminiscent of a subnuclear structure called nuclear speckles (Lamond and Spector, 2003), which is enriched in pre-mRNA processing components and could be identified by the SC-35 antibody. Indeed, Hex1mB2A12.YFP colocalized extensively with the nuclear speckles (Figure 8B, images 1–3). In contrast, it failed to colocalize with two other subnuclear structures, promyelocytic leukemia (PML) nuclear bodies and nucleoli (Figure 8B, images 4–9), which were identified by antibodies directed against the PML and C23 proteins, respectively.

Notably, the C-terminal deletion mutant protein of the Hex1mB2A12.YFP chimera, which lacked the P-TEFb-binding domain (Hex1(1-286)mB2A12.YFP) retained its localization in nuclear speckles (Figure 8C, images 1–3). However, the presence of this C-terminal deletion mutant protein in nuclear speckles *per se* was not sufficient for inhibiting transcription (Figure 8D). Similar to the mutant f.Hex1 protein which failed to bind and inhibit P-TEFb in cells (f.Hex1(1–286); Schulte *et al*, 2005), the mutant f.Hex1mA12 and f.Hex1mB2A12 proteins did not inhibit the activation of transcription by the Gal4.CycT1 chimera (Figure 8D, bars 1–5). Levels of these f.Hex1 chimeras were comparable (Figure 8D, lower panel). Overall, we conclude that AR does not only bind the BR to constitute an inhibitory conformation in HEXIM1. It also mediates HEXIM1 subnuclear localization, since the disruption of AR1 leads to its localization into nuclear speckles, which is a necessary prerequisite for inhibiting transcription.

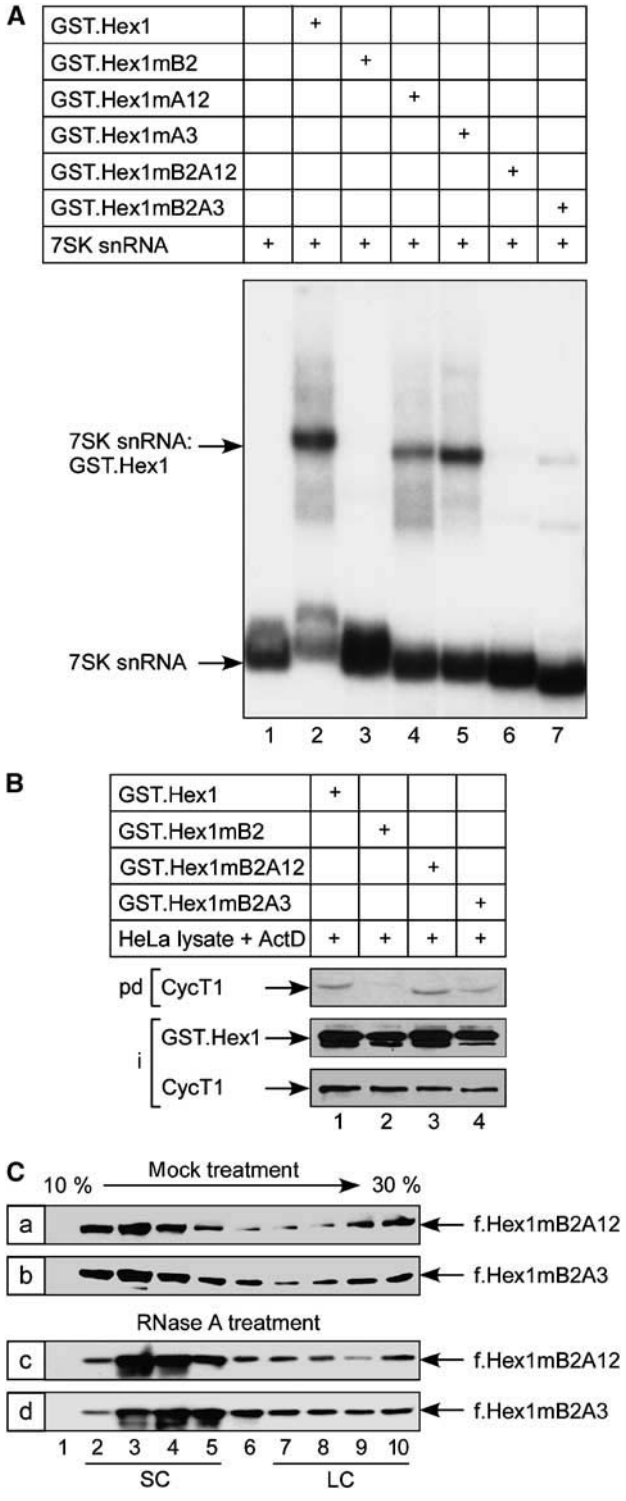

Discussion

By targeting P-TEFb, HEXIM1 inhibits the transcription by RNAPII. In this study, we conducted a comprehensive analysis of the BR and AR in HEXIM1 and provide evidence that these charged regions regulate its function. First, we found that the two monopartite and two bipartite NLSs within the BR in HEXIM1 direct its nuclear import. Second, the evolutionary conserved ARM within the BR1 was essential for the binding between HEXIM1 and 7SK snRNA *in vitro* and for the binding to P-TEFb and inhibition of transcription in cells. Third, BR and AR mediated the interactions between the N- and C-terminal regions of HEXIM1 in the absence of RNA. In addition, the removal of positive or negative charges from these regions alleviated the requirement for the ARM for sequestration of these mutant HEXIM1 proteins into the large complex and their inhibition of transcription. Finally, by removing the negative charges from the AR1 in HEXIM1, its subnuclear localization changed into nuclear speckles. Thus, the interplay between 7SK snRNA and oppositely charged regions in HEXIM1 direct its binding to P-TEFb, subcellular localization, and inhibition of transcription.

Detailed analysis of the BR in HEXIM1, which encompasses only 28 residues, led us to identify four functionally independent NLSs. Since HEXIM1 bound importin α *in vitro* and the monopartite and bipartite NLSs are of the classical type, the HEXIM1 protein is likely to be translocated into the nucleus via the importin α-dependent pathway. However, the presence of ARM within the first monopartite NLS could constitute an arginine-rich NLS, which would bind importin β directly. Such a high number of NLSs in HEXIM1 could ensure its nuclear import in various tissues and organs, since the expression levels of various isoforms of importin α vary in different tissues. Alternatively, various importins may occupy different NLSs at once, leading to a more efficient

Figure 7 The disruption of the AR in HEXIM1 enables the ARM-independent binding to P-TEFb. (**A**) Chimeric GST.Hex1 proteins that were used in EMSAs are indicated above the autoradiograph. α-^{32}P-labeled 7SK snRNA was present in all reactions. Arrows to the left indicate the free 7SK snRNA probe and the presence of 7SK snRNA:GST.Hex1 RNA–protein complexes. (**B**) HeLa cell lysates, which were treated with ActD, were incubated with the chimeric GST.Hex1 proteins as indicated. Arrows to the left indicate bound GST.Hex1 proteins (pd) and 20% inputs (i) of the proteins used in the assay, respectively. (**C**) Total cell lysates of HeLa cells that expressed the indicated f.Hex1 proteins were subjected to glycerol gradient (10–30%) sedimentation analysis. The lysates were mock or RNase A treated as indicated above the Western blots. Arrows to the right indicate the presence of f.Hex1 proteins that were expressed from corresponding plasmid effectors (6 μg). Numberings below the Western blots correspond to particular fractions obtained from the sedimentation analysis. SC and LC indicate fractions containing the small and large complexes, respectively.

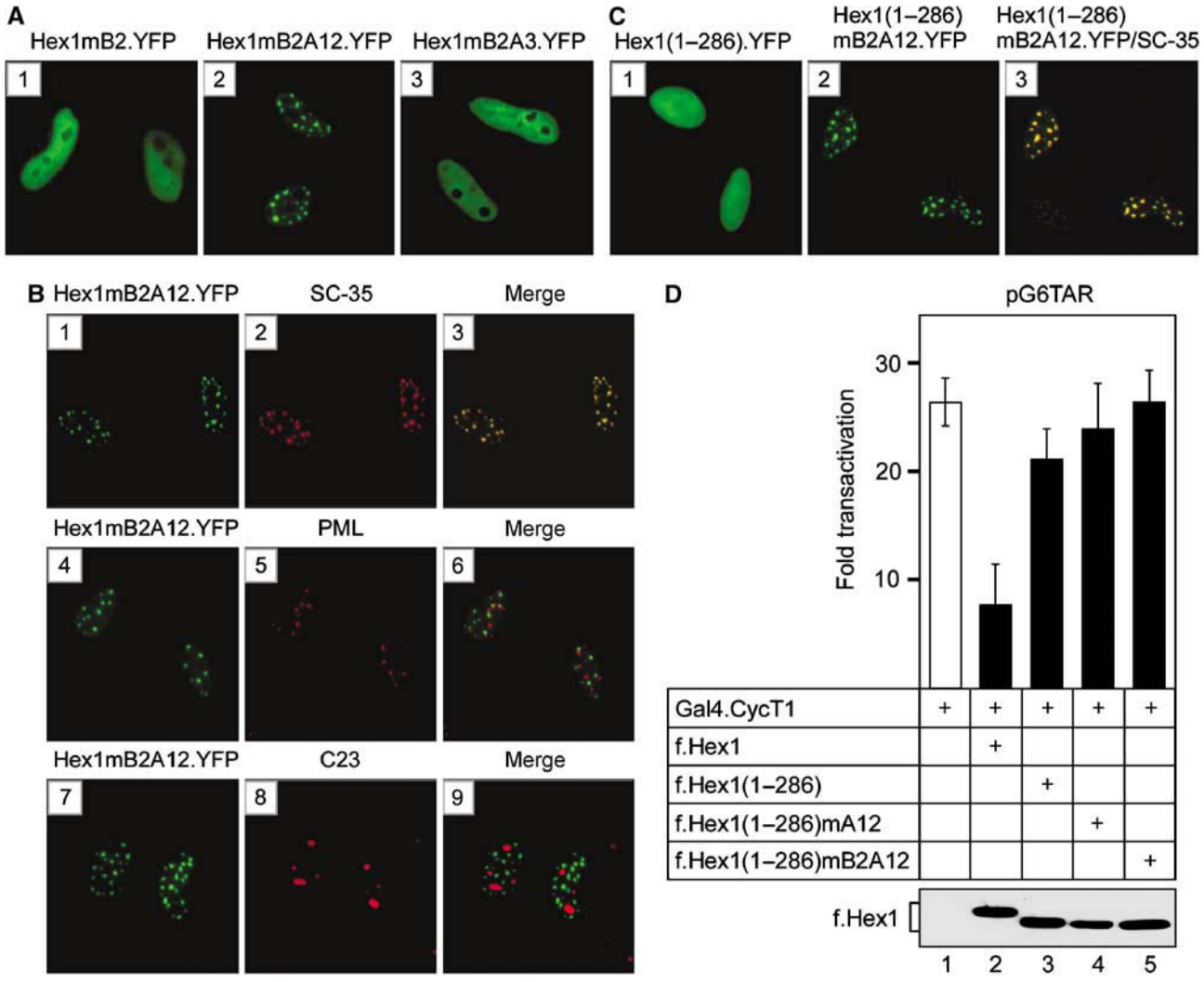

Figure 8 The disruption of the AR1 in HEXIM1 leads to its localization into nuclear speckles. (**A**) Hex1.YFP proteins that were expressed in HeLa cells are indicated above the microscopic images. (**B**) HeLa cells expressed Hex1mB2A12.YFP (green) (images 1–9). The panels marked with SC-35, PML, and C23 (red) represent the images of nuclear speckles, PML nuclear bodies, and nucleoli, whereas the panels marked with merge depict the merge of the Hex1mB2A12.YFP and SC-35, PML, and C23 images, respectively. (**C**) Hex1.YFP proteins (green) that were expressed in HeLa cells are indicated above the microscopic images. The panel marked Hex1(1–286)mB2A12.YFP/C23 depict the merge of the Hex1(1-286)mB2A12.YFP (green) and C23 (red) images. (**D**) HeLa cells expressed plasmid reporter pG6TAR (0.4 μg; bars 1–5). Proteins that were coexpressed from corresponding plasmid effectors (Gal4.CycT1, 0.6 μg; f.Hex1, 0.8 μg) with the plasmid reporter are presented below CAT data. The lower panel presents the expression of f.Hex1 proteins as indicated by the bracket.

nuclear import. Interestingly, when part of the BR.YFP chimera, the ARM constitutes a NoLS. Since nucleoli are dynamic structures with which proteins can associate transiently and under specific metabolic conditions, this finding raises the possibility that the wild-type HEXIM1 protein that resides in the nucleoplasm of HeLa cells under steady-state conditions could be translocated into the nucleolus as well. This is a rather attractive scenario due to the fact that the nucleoli are also sites of RNA modifications (Carmo-Fonseca, 2002), which if operating could regulate its binding to 7SK snRNA.

Recent work demonstrated the critical role for the KHRR motif within the BR in HEXIM1 for its interaction with 7SK snRNA and binding to P-TEFb (Michels *et al*, 2004). Likewise, our EMSAs indicate that the evolutionary conserved ARM is essential for the binding between HEXIM1 and 7SK snRNA *in vitro*. Moreover, the intact ARM is also required for the inhibition of transcription and binding to P-TEFb. On the other hand, we found that the 7SK snRNA interacting surface overlaps with the NLSs and possibly NoLS. This observation is reminiscent of the situation in certain viral RNA-binding proteins. For example, the ARMs in the Tat and Rev proteins of HIV-1, as well as in the Rex protein from the human T-cell leukemia virus type 1, function as effective NLSs and NoLSs (Palmeri and Malim, 1999; Truant and Cullen 1999). Rather than dedicating two separate locations within the protein sequences, HEXIM1 and the viral proteins evolved the same region for these distinct biological functions. Since the bindings to corresponding RNA molecules and importins operate in different locations within cells, namely, in the nucleus and cytoplasm, respectively, these functions are not mutually exclusive. This notion is supported by the mirror image

from the studies investigating the hepatitis delta virus (HDV) antigen (HDAg). One of the biological functions of HDAg is to translocate the HDV RNA genome from the cytoplasm to the nucleus. Beautifully, since both the binding to HDV RNA and importins occur in the cytoplasm, the ARMs and the NLS of the HDAg protein evolved in two separate locations (Chou *et al*, 1998).

How does 7SK snRNA turn HEXIM1 into a P-TEFb inhibitor? Recent reports suggested that 7SK snRNA binds the BR in HEXIM1 to relieve its N-terminal autoinhibitory domain, thus enabling P-TEFb binding (Michels *et al*, 2004; Li *et al*, 2005). Our findings led us to propose a model in which the BR does not only direct the nuclear import of HEXIM1 and its 7SK snRNA binding but could also be involved in establishing an autoinhibitory conformation within the central region of HEXIM1 via its electrostatic interactions with the adjacent AR. According to this scenario, such conformation would be unable to bind P-TEFb unless the 7SK snRNA engaged the BR. Collectively, both models are not mutually exclusive and could therefore operate in concert. For example, we envision a situation where 7SK snRNA would disrupt initially the autoinhibitory conformation in HEXIM1 governed by the centrally located BR and AR, followed by a further conformational change which would reposition the N-terminal autoinhibitory domain and unmask the P-TEFb-binding site. Importantly, both models are consistent by suggesting that the 7SK snRNA releases an autoinhibition of HEXIM1 and that it plays a structural role for the assembly of the inactive complex, rather than contributing directly to P-TEFb inhibition. Notably, by binding the BR, 7SK snRNA facilitates oligomerization of HEXIM1 (Blazek *et al*, 2005). Thus, it is tempting to speculate that this RNA–protein interaction represents a rate-limiting step that could be regulated by at present unknown mechanism and might signify an important checkpoint in determining levels of active and inactive P-TEFb complexes *in vivo*.

Additionally, our study provides exciting observations about the subnuclear localization of HEXIM1 protein. Besides the above-mentioned role of AR in binding the BR and thus disfavoring P-TEFb binding in the absence of 7SK snRNA, we found that the disruption of AR1 within the mutant Hex1.YFPmB2 did not only restore its inhibitory properties by sequestering it into the large complex but also caused its relocalization into nuclear speckles. Consequently, this finding suggests that inhibition of P-TEFb takes place in these subnuclear structures. In support of this conclusion, active transcription does not seem to be associated with nuclear speckles (Cmarko *et al*, 1999). Moreover, a considerable overlap between nuclear speckles and P-TEFb has been documented (Herrmann and Mancini, 2001). Thus, the determination of the subnuclear localization of endogenous components of the complex between 7SK snRNA, HEXIM1, and P-TEFb would be of great interest. Possible perturbations of these localizations, which could result after exposing the cells to various stress-related agents or physiological signals, would provide us further clues about the regulation of this inhibitory complex.

In summary, our study highlights how a plethora of mutually dependent mechanisms meet in a centrally located region in HEXIM1, which in concert with 7SK snRNA directs the sequestration of P-TEFb into the large complex and consequently its catalytic inactivation. In addition, it indicates the importance of intricate subcellular and subnuclear localizations of HEXIM1 that are necessary determinants for exerting its function. Future functional and structural studies will clarify our understanding of HEXIM proteins and uncover the physiological significance of their negative regulation of transcription elongation.

Materials and methods

Cell culture

HeLa cells were grown at 37°C with 5% CO_2 in Dulbecco's modified Eagle's medium (DMEM) containing 10% fetal calf serum, 100 mM L-glutamine, and 50 μg each of penicilin and streptomycin per ml.

Plasmid DNAs

Plasmid reporter pG6TAR and a plasmid coding for the Gal4.CycT1 chimera were described (Taube *et al*, 2002). Plasmids coding for the f.Hex1, f.Hex1(181–359), f.Hex1ΔBR, GST.Hex1, GST.Hex1 (1–180), and h6.x.Impα proteins were gifts from Dr Zhou, Dr Tanaka, and Dr Weis, respectively. Plasmid coding for 7SK snRNA was described (Michels *et al*, 2004). Plasmids coding for the wild-type and mutant f.Hex1, h6.x.Hex1, GST.Hex1, Hex1.YFP, and BR.YFP proteins were generated as described in detail in Supplementary data 3.

Immunoreagents and chemicals

The anti-C23 (nucleolin) (Cat. No. sc-8031, sc-17826), anti-CycT1 (Cat. No. sc-8127), and anti-PML (Cat. No. sc-5621) antibodies were obtained from Santa Cruz Biotechnology (Santa Cruz, CA). The anti-FLAG M2 (Cat. No. F3165), anti-splicing factor SC-35 (Cat. No. S4045) antibodies, and the anti-FLAG M2 beads (Cat. No. FLAGIPT-1) were purchased from Sigma-Aldrich Corp. (St Louis, MO). The anti-Xpress antibody (Cat. No. R910-25) was purchased from Invitrogen (Carlsbad, CA). The secondary anti-mouse or anti-rabbit antibodies conjugated with Alexa fluor 568 or Alexa-flour 488, respectively, were purchased from Invitrogen (Cat. No. A-11019, A-11008; Molecular probes, Carlsbad, CA). The rabbit anti-HEXIM1 antibody was generated against HEXIM1 epitope LHRQQER-APLSKFGD and obtained from Antibody Solutions (Mountain View, CA). Actinomycin D (Cat. No. A 1410) was purchased from Sigma-Aldrich Corp (St Louis, MO).

Transient transfection and CAT reporter gene assay

HeLa cells were seeded into six-well plates or 100-mm-diameter petri dishes approximately 12 h prior to transfection and transfected with FuENE6 reagent (Cat. No. 1 815 091; Roche Applied Science, Indianapolis, IN). CAT enzymatic assays were performed as described (Taube *et al*, 2002). Fold transactivation represents the ratio between the Gal4.CycT1-activated transcription and the activity of the reporter plasmid alone. Error bars give standard errors of the mean.

Immunoprecipitation assay and Western blotting

HeLa cells were lysed in 0.8 ml of lysis buffer A (10 mM Tris–HCl (pH 7.4), 150 mM NaCl, 2 mM EDTA, 1% NP-40, 0.1% protease inhibitor) for 1 h at 4°C 36 h post-transfection. The lysates were immunoprecipitated with the anti-FLAG M2 beads and the bound proteins were separated on SDS–PAGE electrophoresis. Western blotting was performed according to the standard protocols.

Glycerol gradient sedimentation analysis

HeLa cells were lysed in 0.6 ml of lysis buffer B (20 mM HEPES (pH 7.9), 0.3 M KCl, 0.2 mM EDTA, 0.1% NP-40, 0.1% protease inhibitor) containing either 0.5% RNase inhibitor or RNase A (100 μg/ml) for 1 h at 4°C 36 h post-transfection. The lysates were subjected to ultracentrifugation in a SW41 Ti rotor (Beckman) at 38 000 r.p.m. for 16 h in a 10 ml glycerol gradient solution (10–30%) containing buffer B. Fractions were collected and analyzed as described (Yik *et al*, 2005).

Protein purification

Chimeric h6.x.Impα and GST.Hex1 proteins were expressed in the BL21(DE3)pLysS strain of *E.coli* (Novagen, Madison, WI) after a 4 h induction with 1 mM IPTG and purified from total cell lysates by

using Ni-NTA agarose (Qiagen, Chatsworth, CA) and glutathione-Sepharose beads (Amersham Biosciences Corp., Piscataway, NJ), respectively. For EMSAs, purified GST.Hex1 proteins were eluted from the beads by using 20 mM glutathione and 150 mM NaCl in 50 mM Tris–HCl (pH 8.0) and subjected to dialysis against a HGKEDP buffer containing 20 mM HEPES (pH 7.6), 15% glycerol, 50 mM KCl, 0.1 mM EDTA, 1 mM DTT, and 0.1% protease inhibitor. The purity of eluted proteins was determined by silver staining.

In vitro binding assays

For the binding assay between the f.Hex1 proteins and h6.x.Impα, HeLa cells expressed indicated proteins and were lysed in 0.5 ml of lysis buffer A for 1 h at 4°C. Total cell lysates were incubated with equal amounts of the h6.x.Impα protein, coupled to the Ni-NTA agarose beads for 2 h at 4°C. For the GST-pull down assay between GST.Hex1 and h6.x.Hex1 chimeras, the GST.Hex1 proteins were expressed and purified as described above and the mutant h6.x.Hex1 proteins were transcribed and translated *in vitro* using the TNT-T7 Coupled Reticulocyte Lysate System (Cat. No. L4610; Promega Corp., Madison, WI). Each binding reaction was performed in 250 μl of the binding buffer C (20 mM HEPES (pH 7.9), 150 mM KCl, 0.7% β-mercaptoethanol, 0.2% BSA, 0.5% Igepal CA-630 (Cat. No. I-3021; Sigma-Aldrich Corp, St Louis, MO), 1% Triton X-100, 0.1% protease inhibitor) containing either 0.5% RNase inhibitor or RNase A (100 μg/ml) for 2 h at 4°C. For the GST-pull down assay between GST.Hex1 chimeras and P-TEFb, the GST.Hex1 proteins were expressed and purified as described above and P-TEFb was obtained from total HeLa cell lysates which were prepared by treating the HeLa cells with actinomycin D (ActD; 1 μg/ml) for 1.5 h prior to lysis in the lysis buffer D (10 mM HEPES (pH 7.9), 1.5 mM $MgCl_2$, 10 mM KCl, 200 mM NaCl, 0.2 mM EDTA, 0.5% NP-40). Each binding reaction was performed in 300 μl of the buffer D.

EMSA

Reactions (12 μl final) were carried out in 25 mM HEPES (pH 7.6), 15% glycerol, 60 mM KCl, 0.1 mM EDTA, 0.01% NP-40, and 1 μg BSA, and contained 500 pg α-^{32}P-labeled 7SK snRNA and 1 μg poly(I)–poly(C) as a nonspecific competitor RNA. The assay was performed as described (Michels *et al*, 2004).

Immunofluorescence and confocal microscopy

HeLa cell were seeded on cover slips into six-well plates approximately 12 h prior to transfection and transfected with 1 μg of corresponding plasmids as described above. At 24 h after transfection, the cells were fixed with 4% paraformaldehyde and permeabilized in 0.2% Triton X-100 in PBS according to the standard protocols. These steps were followed by incubation with the indicated primary antibodies over night at 4°C. After washing in PBA (PBS + BSA (1 mg/ml)), the cells were incubated for 1 h with the appropriate secondary antibody. Finally, the cells were washed with PBA, incubated with 0.01% PI where indicated in PBS for 10 min, and washed with PBA. Alternatively, the cells were mounted by the ProLong Gold antifade reagent with DAPI (Cat. No. P36935; Molecular Probes, Invitrogen detection technologies, Carlsbad, CA). Confocal microscopy was performed on Zeiss inverted microscope ZW510. Fluorescence of the images containing YFP chimeras was monitored with a Nikon Eclipse E800 microscope using × 40 objective.

Supplementary data

Supplementary data are available at *The EMBO Journal* Online.

Acknowledgements

We thank Q Zhou, JH Yik, H Tanaka, and K Weis for sharing their plasmid reagents, and B Kobe, M Geyer, G Drozina, I Oven, T Vaupotic, and other members of the Peterlin laboratory for help and insightful discussions. This work was supported by a grant from the NIH (PO1 AI058708 from the NIH). MB was supported in part by Grant Number 106584-36-RFNT from the American Foundation for AIDS Research (amfAR).

References

Barboric M, Peterlin BM (2005) A new paradigm in eukaryotic biology: HIV Tat and the control of transcriptional elongation. *PLoS Biol* **3:** e76

Blazek D, Barboric M, Kohoutek J, Oven I, Peterlin BM (2005) Oligomerization of HEXIMI via 7SK snRNA and coiled-coil region directs the inhibition of P-TEFb. *Nucleic Acids Res* (in press)

Byers SA, Price JP, Cooper JJ, Li Q, Price DH (2005) HEXIM2, a HEXIM1 related protein, regulates P-TEFb through association with 7SK. *J Biol Chem* **280:** 16360–16367

Carmo-Fonseca M (2002) The contribution of nuclear compartmentalization to gene regulation. *Cell* **108:** 513–521

Chao SH, Price DH (2001) Flavopiridol inactivates P-TEFb and blocks most RNA polymerase II transcription *in vivo*. *J Biol Chem* **276:** 31793–31799

Chou HC, Hsieh TY, Sheu GT, Lai MM (1998) Hepatitis delta antigen mediates the nuclear import of hepatitis delta virus RNA. *J Virol* **72:** 3684–3690

Cmarko D, Verschure PJ, Martin TE, Dahmus ME, Krause S, Fu XD, van Driel R, Fakan S (1999) Ultrastructural analysis of transcription and splicing in the cell nucleus after bromo-UTP microinjection. *Mol Biol Cell* **10:** 211–223

Dulac C, Michels AA, Fraldi A, Bonnet F, Nguyen VT, Napolitano G, Lania L, Bensaude O (2005) Transcription-dependent association of multiple positive transcription elongation factor units to a HEXIM multimer. *J Biol Chem* **280:** 30619–30629

Herrmann CH, Mancini MA (2001) The Cdk9 and cyclin T subunits of TAK/P-TEFb localize to splicing factor-rich nuclear speckle regions. *J Cell Sci* **114:** 1491–1503

Kusuhara M, Nagasaki K, Kimura K, Maass N, Manabe T, Ishikawa S, Aikawa M, Miyazaki K, Yamaguchi K (1999) Cloning of hexamethylene-bis-acetamide-inducible transcript, HEXIM1, in human vascular smooth muscle cells. *Biomed Res* **20:** 273–279

Lamond AI, Spector DL (2003) Nuclear speckles: a model for nuclear organelles. *Nat Rev Mol Cell Biol* **4:** 605–612

Li Q, Price JP, Byers SA, Cheng D, Peng J, Price DH (2005) Analysis of the large inactive P-TEFb complex indicates that it contains one 7SK molecule, a dimer of HEXIM1 or HEXIM2, and two P-TEFb molecules containing Cdk9 phosphorylated at threonine 186. *J Biol Chem* **280:** 28819–28826

Michels AA, Fraldi A, Li Q, Adamson TE, Bonnet F, Nguyen VT, Sedore SC, Price JP, Price DH, Lania L, Bensaude O (2004) Binding of the 7SK snRNA turns the HEXIM1 protein into a P-TEFb (CDK9/cyclin T) inhibitor. *EMBO J* **23:** 2608–2619

Michels AA, Nguyen VT, Fraldi A, Labas V, Edwards M, Bonnet F, Lania L, Bensaude O (2003) MAQ1 and 7SK RNA interact with CDK9/cyclin T complexes in a transcription-dependent manner. *Mol Cell Biol* **23:** 4859–4869

Nguyen VT, Kiss T, Michels AA, Bensaude O (2001) 7SK small nuclear RNA binds to and inhibits the activity of CDK9/cyclin T complexes. *Nature* **414:** 322–325

Ouchida R, Kusuhara M, Shimizu N, Hisada T, Makino Y, Morimoto C, Handa H, Ohsuzu F, Tanaka H (2003) Suppression of NF-κB-dependent gene expression by a hexamethylene bisacetamide-inducible protein HEXIM1 in human vascular smooth muscle cells. *Genes Cells* **8:** 95–107

Palmeri D, Malim MH (1999) Importin beta can mediate the nuclear import of an arginine-rich nuclear localization signal in the absence of importin alpha. *Mol Cell Biol* **19:** 1218–1225

Sano M, Abdellatif M, Oh H, Xie M, Bagella L, Giordano A, Michael LH, DeMayo FJ, Schneider MD (2002) Activation and function of cyclin T-Cdk9 (positive transcription elongation factor-b) in cardiac muscle-cell hypertrophy. *Nat Med* **8:** 1310–1317

Schulte A, Czudnochowski N, Barboric M, Schonichen A, Blazek D, Peterlin BM, Geyer M (2005) Identification of a cyclin T-binding domain in Hexim1 and biochemical analysis of its binding competition with HIV-1 Tat. *J Biol Chem* **280:** 24968–24977

Sims III RJ, Belotserkovskaya R, Reinberg D (2004) Elongation by RNA polymerase II: the short and long of it. *Genes Dev* **18:** 2437–2468

Taube R, Lin X, Irwin D, Fujinaga K, Peterlin BM (2002) Interaction between P-TEFb and the C-terminal domain of RNA polymerase II activates transcriptional elongation from sites upstream or downstream of target genes. *Mol Cell Biol* **22:** 321–331

Truant R, Cullen BR (1999) The arginine-rich domains present in human immunodeficiency virus type 1 Tat and Rev function as direct importin beta-dependent nuclear localization signals. *Mol Cell Biol* **19:** 1210–1217

Weis K (2003) Regulating access to the genome: nucleocytoplasmic transport throughout the cell cycle. *Cell* **112:** 441–451

Yang Z, Zhu Q, Luo K, Zhou Q (2001) The 7SK small nuclear RNA inhibits the CDK9/cyclin T1 kinase to control transcription. *Nature* **414:** 317–322

Yik JH, Chen R, Nishimura R, Jennings JL, Link AJ, Zhou Q (2003) Inhibition of P-TEFb (CDK9/Cyclin T) kinase and RNA polymerase II transcription by the coordinated actions of HEXIM1 and 7SK snRNA. *Mol Cell* **12:** 971–982

Yik JH, Chen R, Pezda AC, Samford CS, Zhou Q (2004) A human immunodeficiency virus type 1 Tat-like arginine-rich RNA-binding domain is essential for HEXIM1 to inhibit RNA polymerase II transcription through 7SK snRNA-mediated inactivation of P-TEFb. *Mol Cell Biol* **24:** 5094–5105

Yik JH, Chen R, Pezda AC, Zhou Q (2005) Compensatory contributions of HEXIM1 and HEXIM2 in maintaining the balance of active and inactive P-TEFb complexes for control of transcription. *J Biol Chem* **280:** 16368–16376